Effect of Ionic Strength on the Electro-Dipping Force

Galina Lyutskanova–Zhekova[1,2(✉)] and Krassimir Danov[3]

[1] Institute of Mathematics and Informatics,
Bulgarian Academy of Sciences, Sofia, Bulgaria
g.zhekova@math.bas.bg
[2] Faculty of Mathematics and Informatics, Sofia University, Sofia, Bulgaria
[3] Faculty of Chemistry and Pharmacy, Sofia University, Sofia, Bulgaria
kd@lcpe.uni-sofia.bg

Abstract. The calculation of electro-dipping force, acting on a dielectric particle, attached to the boundary between water and nonpolar fluid, is important for the characterization of the surface charge density of micron-size objects and their three-phase contact angles [1]. The problem was solved semi-analytically, using the Mahler–Fox transformation in the simplified case of one phase with infinite dielectric permittivity [4]. We generalize this approach, taking into consideration the finite dielectric permittivity of the polar phase. We propose a numerical method for calculating the distribution of the electrostatic potential in all phases and the respective values of the dimensionless electro-dipping force. The expression for the weak singularity parameter at the three-phase contact line is analytically derived. In all studied cases, it is weaker than that in the model case [2]. The obtained results show that: (i) the electrostatic potential distribution is close to that in the model case for micron-size particles, large values of the ionic strength and dielectric constant of the polar phase; (ii) the force, arising from the electrostatic field in the polar phase, cannot be neglected for small (nano-size) particles and low ionic strengths.

Keywords: Electrostatic potential distribution · Laplace equations
Complex numerical domains and boundary conditions
Toroidal coordinates

1 Introduction

The interactions between electrically charged colloidal particles, adsorbed at an oil–water interface, depend on the magnitude of the surface charge density and the three-phase contact angle. The prediction of the properties of dielectric particles is of crucial importance for the characterization of a particle monolayer,

The work of Galina Lyutskanova–Zhekova has been partially supported by the Sofia University "St. Kl. Ohridski" under contract No. 80-10-139/25.04.2018.

G. Nikolov et al. (Eds.): NMA 2018, LNCS 11189, pp. 433–440, 2019.
https://doi.org/10.1007/978-3-030-10692-8_49

formation of particle-stabilized emulsions and colloidosomes [1]. Experimentally, it has been established that the electrostatic repulsion is due to the presence of charges at the particle–nonpolar phase boundary [2,3].

The problem was solved semi-analytically, using the Mahler-Fox transformation in the simplified case of water phase with infinite dielectric permittivity [4]. The effect of an external electric field, applied to the particle, was discussed in [5]. Our aim in the present study is to analyze the effect of water phase with a finite value of the dielectric constant and to calculate the distribution of the electrostatic potentials in all phases. We solve the Laplace equations in complex physical domains, using appropriate toroidal coordinates. The developed numerical scheme, which is of second order with respect to space and numerical time, allows fast and precise calculations.

2 Mathematical Formulation of the Problem

Let a spherical charged dielectric particle of radius R and dielectric constant ε_{p} is attached to the interface between nonpolar (oil, air) and polar (water) phases with dielectric constants ε_{n} and ε_{w}, respectively (Fig. 1a). The particle position is determined by the central angle α (three-phase contact angle) and therefore the radius of the three-phase contact line is $r_{\mathrm{c}} = R\sin\alpha$. The electric field intensities, $\mathbf{E}_j$ (j = n, p, w), are induced by surface charges of constant surface charge density σ_{pn}, located at the particle–nonpolar phase boundary, S_{pn}. The electric fields in the dielectric phases, occupying volumes V_j (j = n, p, w), obey the equations $\nabla\cdot\mathbf{E}_j = 0$ and the corresponding electrostatic potentials have the form $\mathbf{E}_j = -\nabla\varphi_j$, where ∇ is the gradient operator. Thus, the potentials can be modelled as solutions of the Laplace equations in the volumes, V_j. At the boundaries between water and dielectric phases, S_{pw} and S_{nw}, there are no adsorbed charges, therefore $\varepsilon_{\mathrm{w}}\mathbf{n}\cdot\nabla\varphi_{\mathrm{w}} = \varepsilon_{\mathrm{p}}\mathbf{n}\cdot\nabla\varphi_{\mathrm{p}}$ at S_{pw} and $\varepsilon_{\mathrm{w}}\mathbf{n}\cdot\nabla\varphi_{\mathrm{w}} = \varepsilon_{\mathrm{n}}\mathbf{n}\cdot\nabla\varphi_{\mathrm{n}}$ at S_{nw} hold true, where $\mathbf{n}$ is the outer unit normal vector from the particle surface (Fig. 1a). At the charged part of the particle surface, S_{pn}, we apply the boundary condition $\varepsilon_0\varepsilon_{\mathrm{p}}\mathbf{n}\cdot\nabla\varphi_{\mathrm{p}} - \varepsilon_0\varepsilon_{\mathrm{n}}\mathbf{n}\cdot\nabla\varphi_{\mathrm{n}} = \sigma_{\mathrm{pn}}$, where ε_0 is the dielectric permittivity in vacuum [2,4]. The tangential boundary conditions state that all potentials are continuous functions at the dividing boundaries.

For numerical calculations, it is convenient to reformulate the problem in a dimensionless form. We use the following dimensionless electrostatic potentials, Φ_{p}, Φ_{n}, and Φ_{w}, and ratios between the dielectric constants, $\varepsilon_{\mathrm{pn}}$ and $\varepsilon_{\mathrm{wn}}$:

$$\Phi_j = \frac{\varphi_j\varepsilon_0\varepsilon_{\mathrm{n}}}{r_{\mathrm{c}}\sigma_{\mathrm{pn}}}\ (j = \mathrm{p},\ \mathrm{n},\ \mathrm{w}),\ \varepsilon_{\mathrm{pn}} = \frac{\varepsilon_{\mathrm{p}}}{\varepsilon_{\mathrm{n}}},\ \varepsilon_{\mathrm{wn}} = \frac{\varepsilon_{\mathrm{w}}}{\varepsilon_{\mathrm{n}}}. \tag{1}$$

The cylindrical coordinate system $Or\theta z$ with axis of revolution Oz defines the radial, vertical and polar coordinates, r, z and θ, respectively (Fig. 1a). The complex geometry of the domains is transformed into rectangles (Fig. 1b) by introducing modified toroidal coordinates t and s analogous to those in [2]:

$$\frac{r}{r_{\mathrm{c}}} = \frac{1-t^2}{h},\ \frac{z}{r_{\mathrm{c}}} = \frac{2t\sin s}{h},\ h(t,s) = 1 + t^2 - 2t\cos s. \tag{2}$$

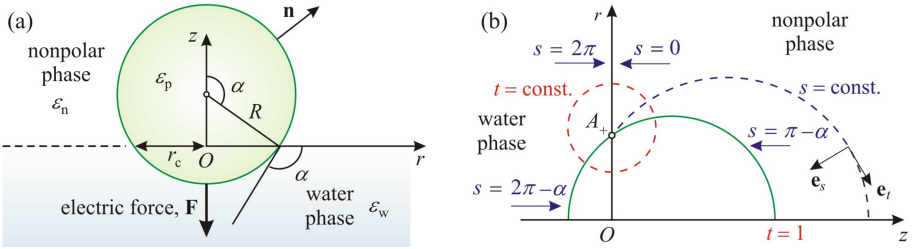

Fig. 1. (a) Sketch of a particle at the interface between nonpolar and water phases. (b) Toroidal coordinate system (t, s), in which the physical domains are transformed into rectangles.

For the curvilinear orthogonal coordinate system, we denote the unit vectors of the local basis by $\mathbf{e}_t$ and $\mathbf{e}_s$. Let us remark that the introduced t and s are similar to the classical toroidal coordinates—we transform the original first coordinate to be in the interval $[0, 1]$. In the new variables, the positions of the interfaces are: $s = 0$ and $s = 2\pi$ from both sides of S_{nw}; $s = \pi - \alpha$ at S_{pn}; $s = 2\pi - \alpha$ at S_{pw}. The axis of revolution corresponds to $t = 1$ and the three-phase contact line—to the pole, A_+, where $t = 0$. The Lamé coefficients, h_t, h_s, and h_θ, of the toroidal coordinate system are calculated from the following relationships:

$$h_t = \frac{2}{h} r_c, \; h_s = \frac{2t}{h} r_c, \; h_\theta = r = \frac{1 - t^2}{h} r_c. \tag{3}$$

Using the general formulae for the Laplace operator and directional derivatives in orthogonal coordinates [2], we get

$$\frac{h}{t(1-t^2)} \frac{\partial}{\partial t} \left[\frac{t(1-t^2)}{h} \frac{\partial \Phi_j}{\partial t} \right] + \frac{h}{t^2} \frac{\partial}{\partial s} \left(\frac{1}{h} \frac{\partial \Phi_j}{\partial s} \right) = 0 \text{ in } V_j \; (j = \text{n,p,w}), \tag{4}$$

$$\mathbf{n} \cdot \nabla u = -\frac{h}{2tr_c} \frac{\partial u}{\partial s} \text{ at } S_{\text{pn}}, \; \mathbf{n} \cdot \nabla u = \frac{h}{2tr_c} \frac{\partial u}{\partial s} \text{ at } S_{\text{pw}}. \tag{5}$$

From the latter, we obtain the dimensionless formulation of the considered problem for the electrostatic potentials: (i) in the volumes—equation (4); (ii) at the dividing physical boundaries:

$$\Phi_{\text{p}}|_{s=2\pi-\alpha} = \Phi_{\text{w}}|_{s=2\pi-\alpha}, \; \varepsilon_{\text{pn}} \frac{\partial \Phi_{\text{p}}}{\partial s}\bigg|_{s=2\pi-\alpha} = \varepsilon_{\text{wn}} \frac{\partial \Phi_{\text{w}}}{\partial s}\bigg|_{s=2\pi-\alpha}, \tag{6}$$

$$\Phi_{\text{n}}|_{s=0} = \Phi_{\text{w}}|_{s=2\pi}, \; \frac{\partial \Phi_{\text{n}}}{\partial s}\bigg|_{s=0} = \varepsilon_{\text{wn}} \frac{\partial \Phi_{\text{w}}}{\partial s}\bigg|_{s=2\pi}, \tag{7}$$

$$\Phi_{\text{n}} = \Phi_{\text{p}}, \; \frac{\partial \Phi_{\text{n}}}{\partial s} - \varepsilon_{\text{pn}} \frac{\partial \Phi_{\text{p}}}{\partial s} = \frac{2t}{1 + t^2 + 2t\cos\alpha} \text{ for } s = \pi - \alpha; \tag{8}$$

(iii) at the axis of revolution, $t = 1$, and at the three-phase contact line, $t = 0$:

$$\frac{\partial \Phi_j}{\partial t} = 0 \text{ for } t = 1 \; (j = \text{n,p,w}), \; \Phi_{\text{n}} = \Phi_{\text{p}} = \Phi_{\text{w}} = 0 \text{ for } t = 0, \tag{9}$$

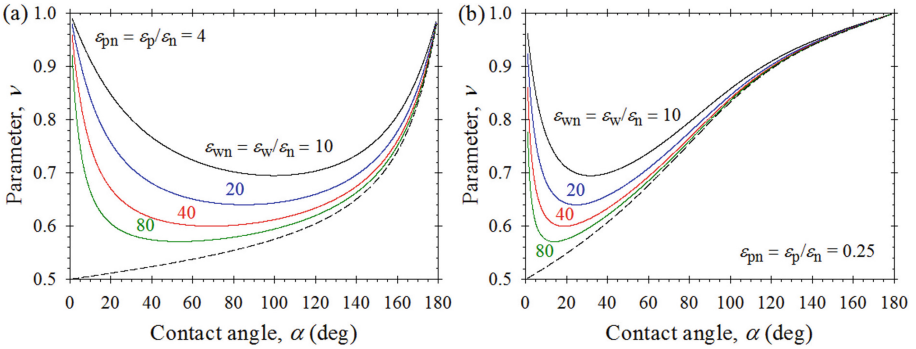

Fig. 2. Dependence of singularity parameter ν on the contact angle α and ratio ε_{wn}: (a) $\varepsilon_{pn} = 4$; (b) $\varepsilon_{pn} = 0.25$. Dashed lines show the model case, studied in [4].

where the electrostatic potentials at the pole A_+ are defined to be equal to zero. It is shown in [4] that the particulate problem has a weak singularity of the electric field intensity in the close vicinity of the contact line. The leading order solutions of Eq. (4) for $t \to 0$ are $\Phi_j = t^\nu (A_j \sin(\nu s) + B_j \cos(\nu s))$, where A_j and B_j (j =n, p, w) are unknown constants and $0.5 < \nu < 1$. The substitution of these solutions into the boundary conditions (6)–(8) leads to a homogeneous system of six linear equations for A_j and B_j. This system has a nontrivial solution, when its determinant is equal to zero. Thus, we arrive to the following equation for the singularity parameter ν:

$$\frac{2\varepsilon_{pn}(1-\varepsilon_{wn})^2}{(1+\varepsilon_{pn})(1+\varepsilon_{wn})(\varepsilon_{pn}+\varepsilon_{wn})} - \sin^2(\nu\pi) = \frac{(1-\varepsilon_{pn})(1-\varepsilon_{wn})}{(1+\varepsilon_{pn})(1+\varepsilon_{wn})}\cos^2(\nu\alpha) + \frac{(1-\varepsilon_{wn})(\varepsilon_{pn}-\varepsilon_{wn})}{(1+\varepsilon_{wn})(\varepsilon_{pn}+\varepsilon_{wn})}\cos^2\left[\nu(\pi-\alpha)\right]. \qquad (10)$$

The model case, studied in [4], follows from (10) when $\varepsilon_{wn} \to \infty$ (dashed lines in Fig. 2). The solutions of Eq. (10) for the singularity parameter, ν, for two different ratios ε_{pn} are shown in Fig. 2. The following conclusions can be drawn from it. In all cases, the singularity is weaker than that in the model case. The values of ν increase with the decrease of the ratio between the dielectric constants of water and nonpolar phase, ε_{wn}. This effect is more pronounced for larger values of ε_{wn} and more hydrophilic particles.

3 Numerical Method

In order to find a numerical solution of the problem, we apply the alternating direction implicit method (ADIM), introducing numerical time τ. The continuous function $f(\tau, t, s)$ describes the electrostatic potentials, ordered as follows:

$\Phi_{\rm n}$, $\Phi_{\rm p}$, and $\Phi_{\rm w}$. In the volumes, $f(\tau, t, s)$ obeys an equation of the form (4):

$$\frac{\partial f}{\partial \tau} = \mathbf{T}[f] + \mathbf{S}[f],$$
$$\mathbf{T}[f] = \frac{h}{t(1-t^2)}\frac{\partial}{\partial t}\left[\frac{t(1-t^2)}{h}\frac{\partial f}{\partial t}\right],\ \mathbf{S}[f] = \frac{h}{t^2}\frac{\partial}{\partial s}\left(\frac{1}{h}\frac{\partial f}{\partial s}\right), \tag{11}$$

where the operators $\mathbf{T}$ and $\mathbf{S}$ act in directions t and s, respectively. For the discretization of (11), we introduce an uniform mesh with time step δ_τ and space steps δ_n, δ_p, δ_w by dividing each numerical domain $\tilde{V}_j$ $(j = n, p, w)$ into squares of length δ_j. We denote the solution at a given moment τ by subscript "0" and at the moment $\tau + 2\delta_\tau$—by subscript "2". Using the Crank–Nicolson method in the ADIM scheme, we obtain the following second order numerical model:

$$(\mathbf{U} - \delta_\tau \mathbf{S})(\mathbf{U} - \delta_\tau \mathbf{T})[f_2 - f_0] = 2\delta_\tau \mathbf{T}[f_0] + 2\delta_\tau \mathbf{S}[f_0] + O(\delta_\tau^3), \tag{12}$$

where $\mathbf{U}$ is the unit operator. Firstly, we solve numerically an equation for a function $g(t, s)$ in the s-direction, and subsequently—an equation in the t-direction

$$(\mathbf{U} - \delta_\tau \mathbf{S})[g] = 2\delta_\tau \mathbf{T}[f_0] + 2\delta_\tau \mathbf{S}[f_0] \text{ and } (\mathbf{U} - \delta_\tau \mathbf{T})[f_2 - f_0] = g \tag{13}$$

as the derivatives in $\mathbf{T}$ and $\mathbf{S}$ are approximated with second-order central differences with respect to t and s.

The main problem in the ADIM arises from the complexity of the boundary conditions, applied to the function g. In order to have a second order precision with respect to t and s, we modify the boundary conditions, assuming the validity of the Laplace equations in the close vicinity of the dividing surfaces and the axis of revolution [6]. We use the following approximation:

$$u''(x) = \frac{-7u(x) + 8u(x \pm \delta_x) - u(x \pm 2\delta_x)}{2\delta_x^2} \mp \frac{3}{\delta_x}u'(x) + O(\delta_x^2), \tag{14}$$

which relates the second and the first derivative of a given function. For example, the limit of the operator $\mathbf{T}$ at the axis of revolution, taking into account the boundary conditions (9) and equation (11), yields

$$\lim_{t\to 1} \mathbf{T}[u] = 2\left.\frac{\partial^2 u}{\partial t^2}\right|_{t=1} = \frac{-7u(1) + 8u(1-\delta_t) - u(1-2\delta_t)}{2\delta_t^2}. \tag{15}$$

Therefore, we replace the boundary conditions (9) with Eq. (13), in which the operator $\mathbf{T}$ is given by the difference form (15). The result is a modified boundary condition in relaxed form.

From Eqs. (11) and (14), the finite difference representations of the operator $\mathbf{S}$ in the close vicinity of the boundary $s = \pi - \alpha$ are

$$t^2 a_{\rm n}\mathbf{S}[u] = \frac{-7u(s) + 8u(s-\delta_{\rm n}) - u(s-2\delta_{\rm n})}{2\delta_{\rm n}^2}a_{\rm n} + u'(s-0), \tag{16}$$

$$t^2 a_{\rm p}\mathbf{S}[u] = \frac{-7u(s) + 8u(s+\delta_{\rm p}) - u(s+2\delta_{\rm p})}{2\delta_{\rm p}^2}a_{\rm p} - \varepsilon_{\rm pn}u'(s+0), \tag{17}$$

where the functions $a_{\mathrm{n}}(t)$ and $a_{\mathrm{p}}(t)$ are defined with

$$a_{\mathrm{n}}(t) = \delta_{\mathrm{n}} \left(3 - \frac{\delta_{\mathrm{n}}}{h}\frac{\partial h}{\partial s}\right)^{-1}, \; a_{\mathrm{p}}(t) = \varepsilon_{\mathrm{pn}}\delta_{\mathrm{p}} \left(3 + \frac{\delta_{\mathrm{p}}}{h}\frac{\partial h}{\partial s}\right)^{-1} \text{ for } s = \pi - \alpha. \quad (18)$$

The sum of Eqs. (16) and (17) along with the boundary conditions (8) leads to the final expression for the finite difference form of the operator **S** at the boundary S_{pn}:

$$\mathbf{S}[u] = \frac{-7u(s) + 8u(s - \delta_{\mathrm{n}}) - u(s - 2\delta_{\mathrm{n}})}{2\delta_{\mathrm{n}}^2 t^2 (a_{\mathrm{n}} + a_{\mathrm{p}})} a_{\mathrm{n}}$$
$$+ \frac{-7u(s) + 8u(s + \delta_{\mathrm{p}}) - u(s + 2\delta_{\mathrm{p}})}{2\delta_{\mathrm{p}}^2 t^2 (a_{\mathrm{n}} + a_{\mathrm{p}})} a_{\mathrm{p}} + \frac{2}{ht(a_{\mathrm{n}} + a_{\mathrm{p}})} \text{ for } s = \pi - \alpha. \quad (19)$$

Thus, the boundary conditions (8) are replaced by Eq. (13), in which the operator **S** is given by definition (19). Following an analogous procedure, we derive the respective expression for the difference form of **S** at the boundary $s = 2\pi - \alpha$ and on both sides of S_{nw} ($s = 0$ and $s = 2\pi$).

Because of the boundary conditions, the considered algorithm reduces the matrix of the linear algebraic system in the t-direction to a five-diagonal matrix. The respective matrix of the system in the s-direction is again with five non-zero diagonals, but because of the periodicity of the solution at S_{nw} its first row contains two more elements at the end and the last row contains two more elements at the beginning. We implemented a direct elimination numerical method in order to solve the system.

4 Results and Discussion

To achieve good precision of the numerical calculations, we discretize each numerical domain $\tilde{V}_j$ (j = n, p, w) by introducing a 100×100 uniform mesh (see Sect. 3). The time step is chosen to be equal to the minimum of δ_{n}, δ_{p} and δ_{w}. The illustrative figures (Figs. 3b and 4b) correspond to experimental system parameters [2] $\varepsilon_{\mathrm{pn}} = 2$ and $\varepsilon_{\mathrm{wn}} = 40$. If the oil phase has a larger dielectric constant (for example, castor oil with $\varepsilon_{\mathrm{n}} = 4.54$), then the system parameters are $\varepsilon_{\mathrm{pn}} = 0.874$ and $\varepsilon_{\mathrm{wn}} = 17.2$ (Figs. 3a and 4a, respectively). The mathematical formulation of the problem assumes that the electrostatic potential at the three-phase contact line is equal to zero (see Eq. (9)) and the intensity of the electric field at large distances from the charged particle is equal to zero. Thus, the calculated potential at infinity has a non-zero value. It is subtracted from the calculated Φ_j in order to obtain the physical electrostatic potential.

Figure 3 shows the distribution of the physical values of Φ_j in the numerical domains for three-phase contact angle $\alpha = 90°$. The considerably higher dimensionless potentials are well illustrated for larger values of the dielectric constant of the nonpolar phase. At the coordinate lines, $s = 0$ (S_{nw}) and $s = 3\pi/2$ (S_{pw}), the electrostatic potentials are considerably lower than those at coordinate line

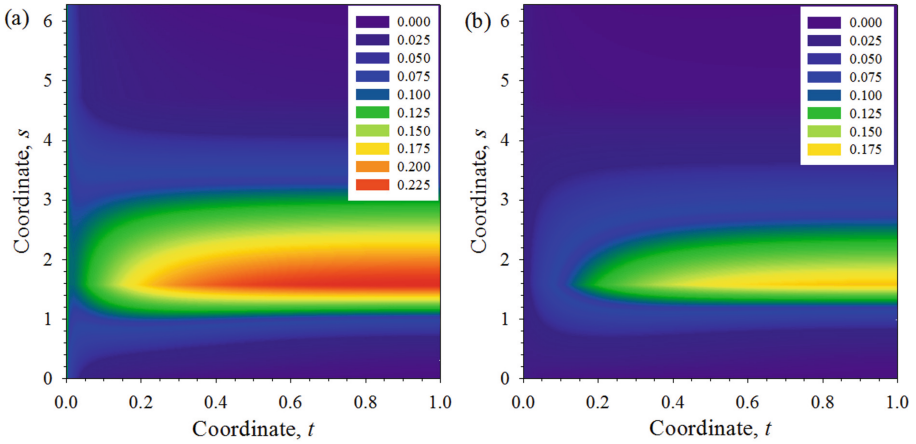

Fig. 3. Distribution of the electrostatic potentials in numerical domains for contact angle $\alpha = 90°$: (a) $\varepsilon_{pn} = 0.874$ and $\varepsilon_{wn} = 17.2$; (b) $\varepsilon_{pn} = 2$ and $\varepsilon_{wn} = 40$.

$s = \pi/2$ (S_{pn}). As it can be expected, the maxima of the electrostatic potentials are at the cross-section of the particle–nonpolar interface and the axis of revolution. The dielectric constant of water is so high that the water phase suppresses the penetration of the electric field in polar phase.

The calculations in [2,4] are performed, assuming zero values of the potentials at the boundaries of the polar fluid. The magnitude of the electro-dipping force decreases if the electrostatic potentials of these boundaries are different than zero. Figure 4 shows the distribution of the surface potentials along the boundaries (solid lines correspond to S_{pn}; dashed lines to S_{pw}; dot-dashed lines — to S_{nw}). The increase of the three-phase contact angle (more hydrophobic particles) leads to higher potentials because of the more charges adsorbed at the particle–nonpolar fluid interface. The effect of the water phase becomes more

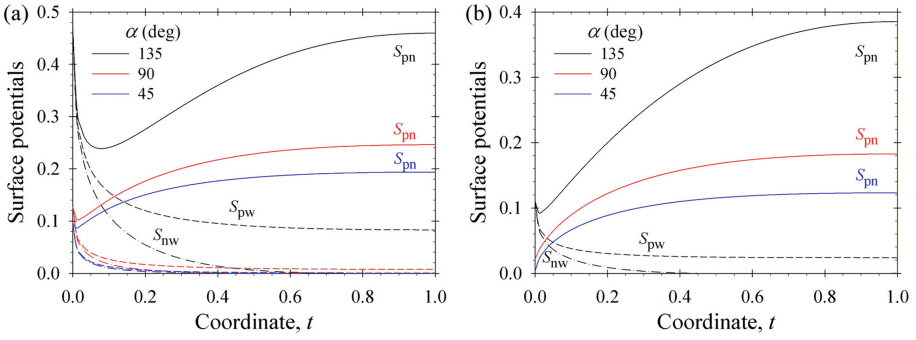

Fig. 4. Distribution of potentials along the interfaces for different values of contact angle α: (a) $\varepsilon_{pn} = 0.874$ and $\varepsilon_{wn} = 17.2$; (b) $\varepsilon_{pn} = 2$ and $\varepsilon_{wn} = 40$.

pronounced. It is important to note that the surface potentials at the particle–water boundary are different from zero. Thus, the boundary S_{pw} also contributes to the electro-dipping force. For $\alpha = 45°$ and $\alpha = 90°$ this contribution is small, while for $\alpha = 135°$ — it is not negligible. The weak singularities at the three-phase contact line ($t = 0$) correspond to those depicted in Fig. 2. If the dielectric constant of the particle phase, ε_{p}, is smaller than that of the nonpolar phase, ε_{n}, then the electric field penetration inside the particle phase is more effective and the electrostatic potential at boundary S_{pw} is higher.

5 Conclusions

The developed effective numerical algorithm, based on the ADIM scheme, gives possibility for fast and precise calculation of the distributions of electrostatic potentials, generated from a charged dielectric particle, attached to the nonpolar–water interface. For faster calculations, the complex numerical domains are transformed into rectangles, using appropriate toroidal coordinates. The resulting cyclic five diagonal systems of linear equations in the respective directions of ADIM are solved, using a direct elimination method.

The numerical results show the effect of the three-phase contact angle and the dielectric properties of the phases on the induced electric fields and the magnitude of the electro-dipping force. Generally, the decrease of the ratios of the dielectric constants of the particle and nonpolar phase, $\varepsilon_p/\varepsilon_{\mathrm{n}}$, and that of water and nonpolar phase, $\varepsilon_{\mathrm{w}}/\varepsilon_{\mathrm{n}}$, leads to the more pronounced penetration of electric field and higher surface potentials at the particle–water and nonpolar fluid–water boundaries. The magnitude of the potentials (electro-dipping force) is larger for more hydrophobic particles. The calculations generalize what is known from literature [2,4] and give a more precise description of the problem.

References

1. Lotito, V., Zambelli, T.: Approaches to self-assembly of colloidal monolayers: a guide to nanotechnologists. Adv. Colloid Interface Sci. **246**, 217–274 (2017)
2. Danov, K., Kralchevsky, P., Boneva, M.: Electrodipping force acting on solid particles at a fluid interface. Langmuir **20**(15), 6139–6151 (2004)
3. Horozov, T., Aveyard, R., Binks, P., Clint, J.: Structure and stability of silica particle monolayers at horizontal and vertical octane-water interfaces. Langmuir **21**(16), 7405–7412 (2005)
4. Danov, K., Kralchevsky, P.: Electric forces induced by a charged colloid particle attached to the water-nonpolar fluid interface. J. Colloid Interface Sci. **298**(1), 213–231 (2006)
5. Danov, K., Kralchevsky, P.: Forces acting on dielectric colloidal spheres at a water/nonpolar fluid interface in an external electric field. 2. charged particles. J. Colloid Interface Sci. **405**, 269–277 (2013)
6. Wang, Y., Wang, T.: A compact ADI method and its extrapolation for time fractional sub-diffusion equations with nonhomogeneous Neumann boundary conditions. Comput. Math. Appl. **75**(3), 721–739 (2018)